JOURNAL OF VIROLOGY, Feb. 1989, p. 1002–1006
0022-538X/89/021002-05$02.00/0

Vol. 63, No. 2

Evidence for a Ligation Step in the DNA Replication of the Autonomous Parvovirus Minute Virus of Mice

SUSAN F. COTMORE,[1] MAGALI GUNTHER,[2]† AND PETER TATTERSALL[1,2]*

Departments of Laboratory Medicine[1] and Human Genetics,[2] Yale University School of Medicine, 333 Cedar Street, New Haven, Connecticut 06510

Received 15 August 1988/Accepted 24 October 1988

Newly replicated DNA of the autonomous parvovirus minute virus of mice was pulse-labeled with $^{32}PO_4$ during the time of maximal viral DNA replication in highly synchronized A9 cells. The subsequent processing of viral DNA-protein complexes was monitored during a chase period with no label. Several distinct classes of duplex replicative-form and progeny single-stranded DNA molecules were characterized and found to accumulate at different times during infection. Analysis of the terminal structures associated with these various forms provided new insights into the mechanism by which viral DNA replicates and, in particular, suggested that interstrand ligation occurs during this process.

Virions of the autonomous parvovirus minute virus of mice (MVM) contain a single copy of a linear, nonpermuted, negative-sense DNA molecule of approximately 5 kilobases in which a long, single-stranded coding region is bracketed by short terminal palindromic sequences capable of folding into hairpin duplexes (4). Analysis of defective interfering particles has shown that all of the *cis*-acting information necessary for viral DNA replication and encapsidation resides within 250 nucleotides of each telomere (7), and thus all models of MVM replication focus on explaining their regeneration. The original rolling hairpin model invoked a system of self-priming at the genomic termini, coupled with a hairpin transfer mechanism which copied the palindromic sequence at the 5′ end of one strand onto the 3′ end of its complement (11). While many predictions of the original model have been confirmed, detailed sequence analysis of the left-hand (3′) ends of viral sense strands indicated that a more complex mechanism might be required for their regeneration (1, 2). These termini are imperfect palindromes, containing a few asymmetrical nucleotides which are mispaired in the hairpin form. The presence of these mismatched residues allows identification of two sequence orientations, termed "flip" and "flop," in the right-hand termini of both viral and replicative-form (RF) molecules of MVM, as would be expected from such a hairpin transfer mechanism. However, only a single sequence orientation is present in the left-hand terminus of either type of DNA molecule.

To explain how this sequence orientation could be conserved, Astell and colleagues (1, 2) proposed that the left-hand end of the viral genome might be excised from a dimer duplex RF DNA molecule by an enzyme which would recognize and bind to the palindromic sequence present in only one strand of the duplex. They proposed that this enzyme might function in a manner analogous to that described for the topoisomerase encoded by the *A* gene of bacteriophage φX174 (6, 9), splitting a phosphodiester bond in the DNA in a site-specific manner and forming a covalent bond with the 5′-phosphoryl group at the nick site (10, 12), thus conserving the energy of the cleaved phosphodiester bond. Following translocation along the strand (by displacement synthesis), a second active site in the same protein could then introduce a second nick, this time into the complementary strand, at a second copy of its specific cutting site. In doing so it would establish a covalent bond with the new 5′ end and liberate a 3′-hydroxyl group capable of attacking the original 5′-phosphoryl DNA-protein linkage. This would create one "turn-around" terminus by ligating the two DNA strands and one "extended" terminus bearing the enzyme covalently attached to its 5′ end. Such a mechanism would generate a single sequence orientation at all left-hand termini, while right-hand termini, which are generated as both flip and flop forms in vivo, could be cut from molecules in the turn-around configuration, provided that both the binding and cutting sites for the enzyme were available in this structure.

Acceptance of this replication scheme demands detailed corroborative evidence, particularly since it is not immediately obvious what advantage such a complex mechanism might provide for the virus. We recently showed that the major viral nonstructural protein, NS-1, is covalently attached to the 5′ termini of all newly synthesized duplex RF and progeny single-stranded DNA molecules (5, 7a). According to the modified rolling hairpin model proposed by Astell and colleagues (1, 2), this association implicates NS-1 as the topoisomerase involved in excising both right- and left-hand genomic termini. The experiments presented in this paper identify several different forms of monomer and dimer duplex RF molecules, with different terminal configurations, which are generated during the course of infection, and these observations allow us to reevaluate the existing models of viral DNA replication in terms of their ability to explain the structures generated in vivo.

Generation of three discrete forms of monomer RF, three forms of dimer RF, and two forms of progeny single-stranded DNA during the course of infection. Total-cell extracts were obtained from highly synchronized, MVM-infected A9 cells which had been pulse-labeled with $^{32}P_i$ for 1 h starting 10 h after the onset of S phase and then harvested immediately (Fig. 1A, lane 1) or chased with unlabeled phosphate for 1 h (Fig. 1A, lane 2), 2 h (Fig. 1A, lane 3), or 14 h (Fig. 1A, lane 4) as previously described (5). This double-block synchronization procedure, which is adapted from the technique of Heintz and colleagues (8), uses 48 h of isoleucine deprivation followed by exposure to MVM in the presence of the alpha

* Corresponding author.
† Present address: Laboratoire de Biochimie, Section de Biologie, Institut Curie, Paris Cedex 05, France.

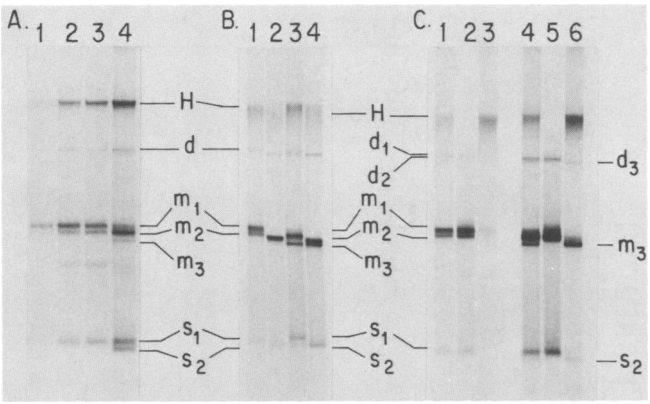

FIG. 1. (A) Autoradiograph of a 1% agarose–SDS gel showing total-cell extracts from highly synchronized A9 cells infected with MVM and labeled with $^{32}P_i$ (500 μci/ml at 1/20th the normal PO_4 concentration) for 1 h beginning 10 h after release from aphidicolin, and harvested immediately (lane 1) or chased with unlabeled medium for 1 h (lane 2), 2 h (lane 3), or 14 h (lane 4). (B) Effect of proteinase K digestion. Lanes: 1 and 3, total-cell extracts identical to those in panel A, lanes 2 and 4, respectively; 2 and 4, proteinase K digests (100 μg of proteinase K per ml for 30 min) of the same extracts. (C) Total-cell extracts from MVM-infected cells pulsed with $^{32}P_i$ as described above and chased with unlabeled medium for 1 h (lane 1) or 14 h (lane 4), together with the material immunoprecipitated from these extracts with a monospecific antibody (3) directed against the virally encoded NS-1 molecule (lanes 2 and 5, respectively) and the material remaining unbound after such a precipitation (lanes 3 and 6, respectively). Discrete monomer duplex RF species are labeled m1, m2, and m3, while dimer RF species are labeled d (in panels A and B) or d1, d2, and d3 (in panel C). Two forms of progeny single-stranded DNA are designated s1 and s2. H, High-molecular-weight host DNA.

and delta DNA polymerase inhibitor aphidicolin for 20 h. Removal of the inhibitor allows the initiation of cellular S phase which, in infected cells, is followed 8 to 12 h later by viral duplex DNA amplification and progeny single-stranded DNA synthesis (4). Thus, in the experiments presented here, cells were labeled and the first samples were collected during the peak period of viral DNA synthesis, whereas those samples collected 25 h after the start of the S phase (Fig. 1A, lane 4) were from cells approaching the end of a single cycle of viral growth. Throughout the first 3 h of the analysis, most of the label was associated with a particular form of monomer RF, designated m1, although a second, faster-migrating form of monomer RF, designated m2, was also present at all times (Fig. 1A). Quantitation of the two bands during the first 2 h of the experiment indicated that the ratio of m1 to m2 remained relatively constant at this time, but by 13 h after the start of S phase (Fig. 1A, lane 3), the ratio was beginning to change, and by the end of the replication cycle (Fig. 1A, lane 4), the m2 form predominated and a third, faster-migrating form of monomer RF, designated m3, had begun to accumulate. Labeled single-stranded DNA (s1) and dimer duplex RF (d) were also present in all the extracts shown in Fig. 1, although they could not be seen in all the samples at this autoradiographic exposure. These forms also appeared to accumulate with increasing chase times. In addition, new, faster-migrating forms of single-stranded DNA (s2) and dimer RF (d3) accumulated after the extended chase (Fig. 1).

Pulse-chase experiments carried out with $^{32}P_i$ are complicated by the presence of a labeled nucleotide pool which is generated during the pulse period and remains available for de novo strand synthesis at the beginning of the chase period. The extent to which this pool complicates interpretation of the experiment presented in Fig. 1 can be assessed by comparing the absolute amounts of labeled DNA seen in Fig. 1A, lanes 1 through 4. Clearly, during the first hour of the chase period this de novo incorporation was substantial, but at later times relatively little new isotope was incorporated; thus, despite some continued labeling of newly synthesized strands, this type of analysis does predominantly monitor the modification of preexisting DNA forms. When continuous-pulse experiments were used to examine total viral DNA synthesized during the course of a similar infection, essentially the same DNA forms were observed. Thus, by 25 h after the start of S phase, the m2 and m3 forms of monomer RF predominated over the m1 form, and faster-migrating forms of dimer duplex RF and single-stranded DNA were abundant (data not shown). However, such results were less visually accessible because of the massive accumulation of progeny single-stranded DNA synthesized over time. In contrast, in the pulse-chase samples shown here, one-half of the incorporated label was presumably in complementary-sense DNA and thus was permanently trapped in the residual duplex structures.

When pulse-chase-labeled extracts were digested with proteinase K, forms m1 and m2 collapsed to produce a new band with an electrophoretic mobility between that of m2 and m3 (Fig. 1B, compare lane 1 with lane 2 and lane 3 with lane 4), while the mobility of m3 remained unchanged (Fig. 1B, lane 4). Proteolysis also affected the s1 form of single-stranded DNA, leaving a deproteinized molecule which exactly comigrated with the s2 form (Fig. 1B, lanes 2 and 4).

The viral DNA forms present during the first 3 h of the experiment could be immunoprecipitated almost quantitatively from extensively denatured cell extracts with antisera directed against the virally coded NS-1 molecule (Fig. 1C), as previously described (5). In contrast, the new forms of monomer (m3), dimer (d3), and single-stranded (s2) DNA molecules generated later in the infection were not associated with NS-1 (Fig. 1C, lane 6).

Analysis by alkaline SDS gel electrophoresis and exonuclease digestion. Pulse-chase-labeled samples were also analyzed on fully denaturing alkaline agarose gels run in the presence of sodium dodecyl sulfate (SDS). Extracts harvested after a 1-h chase resolved into a major single-stranded DNA band at around 5 kilobases (kb) and another at around 10 kb, designated 5+ and 10+, respectively (Fig. 2, lane 1). Samples harvested after the 14-h chase period, however, produced a more complex pattern (Fig. 2, lane 2) containing the 5+ and 10+ bands seen in the previous sample as well as faster-migrating species, designated 5− and 10−, respectively, at each of these positions and a new form, designated mC, which migrated at around 13 kb in this gel. Proteinase K digestion increased the mobility of bands 5+ and 10+ (Fig. 2, lane 3), indicating that these forms were complexed with protein, a conclusion which was confirmed by the fact that they could be immunoprecipitated with anti-NS-1 serum (Fig. 2, lane 4). When such immunoprecipitates were digested with proteinase K prior to electrophoresis, the mobilities of both the 5+ and 10+ kb single-stranded forms increased (Fig. 2, lane 5), confirming that the observed protein-DNA linkage was resistant to the denaturing alkaline conditions used in this gel. The mobilities of bands 5−, 10−, and mC did not change after proteinase K digestion (Fig. 2, lane 3), and these forms remained in the unbound material left after anti-NS-1 immunoprecipitation (Fig. 2, lane 6), indicating that they corresponded to the d3, m3, and s2 forms identified in Fig. 1.

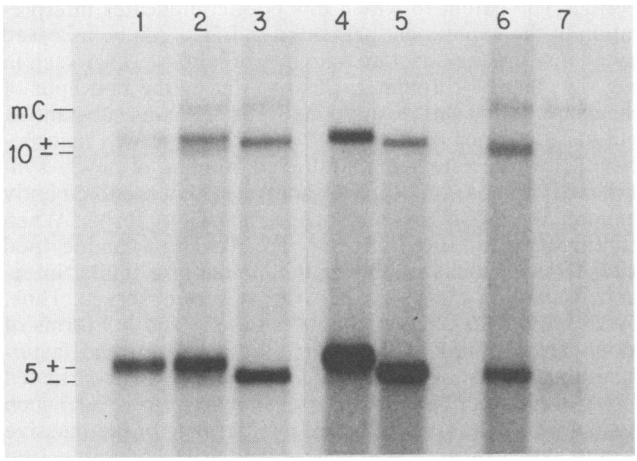

FIG. 2. Autoradiograph of a denaturing alkaline 1% agarose–SDS gel showing total-cell extracts from cells pulsed with $^{32}P_i$ for 1 h starting 10 h after the start of S phase and then chased with cold medium for 1 h (lane 1) or 14 h (lane 2). Samples of the extract shown in lane 2 were digested with proteinase K to yield the species shown in lane 3 or fractionated by immunoprecipitation with antiserum directed against the MVM NS-1 molecule to yield both the antibody-bound species shown in lane 4 and the unbound fraction shown in lane 6. A sample of antibody-bound DNA identical to that shown in lane 4 but digested with proteinase K is shown in lane 5. Lane 7 shows a sample of the unbound fraction from lane 6 following digestion with 25 U of exonuclease III for 30 min. Two forms of single-stranded DNA with lengths of about 10 kb are designated 10+ and 10−, two forms of single-stranded DNA with lengths of about 5 kb are designated 5+ and 5−, and a proteinase K- and exonuclease III-resistant species which migrated at about 13 kb is designated mC.

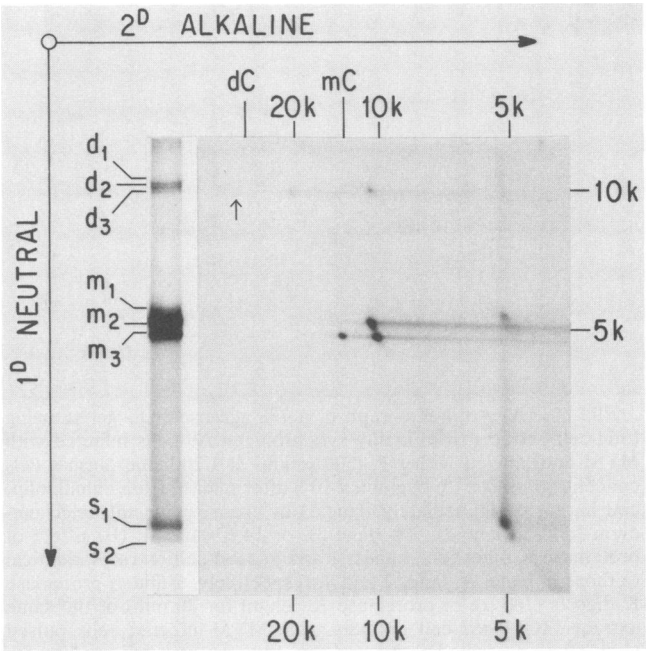

FIG. 3. Autoradiograph of a two-dimensional 1% agarose–SDS gel showing total-cell extracts from highly synchronized cells labeled with $^{32}P_i$ between 10 and 11 h after the start of the S phase, chased with unlabeled medium for 14 h, and analyzed first under neutral (1^D) conditions and then under alkaline (2^D) conditions. Single-stranded DNA forms (s1 and s2), which migrated as collapsed rods in the neutral dimension, migrated as molecules of around 5 kb in the alkaline gel and comigrated in this dimension with the upper (m1) forms of monomer duplex DNA. In contrast, m2 forms migrated as 10-kb single strands in the second dimension, indicating that they have a turn-around sequence at one end and an extended sequence at the other. The m3 forms migrated either as 10-kb single strands or with a higher mobility, consistent with their being circular molecules in which both termini are in the covalently closed turn-around configuration (mC). Four analogous forms of dimer duplex DNA were also apparent: d1, which migrated in the alkaline dimension as 10-kb single strands (i.e., it had no turn-around termini); d2, which migrated as a 20-kb single strand (i.e., it had one turn-around terminus per molecule); and d3, which migrated as 20-kb linear molecules or as 20-kb circular molecules (dc indicated by arrow). k, Kilobases.

Band mC was of particular interest because its apparent molecular weight varied significantly with the agarose concentration of the gel in which it was analyzed (data not shown), a feature characteristic of circular single strands. To explore the possibility that the mC form was indeed a single-stranded circle, DNA remaining unbound after immunoprecipitation with anti-NS-1 antibody was digested with exonuclease III prior to denaturation. This duplex-dependent, 3′-to-5′ exonuclease destroyed the 10− band, reducing it to a smear at around 5 kb (Fig. 2, lane 7), and destroyed the original 5− band, reducing it to an even broader smear at around 2.5 kb (data not shown). However, exonuclease III digestion did not affect the mC band, strongly supporting the contention that this molecule is a covalent continuous form of monomer RF. Similar experiments (not shown) with bacteriophage lambda exonuclease, which has a 5′-to-3′ specificity, were complicated by the fact that essentially every "correct" 5′ end in duplex viral DNA is occupied by an NS-1 molecule (5).

Two-dimensional SDS-agarose gel electrophoresis. To explore further the nature of the various monomer and dimer forms of RF DNA, we performed two-dimensional electrophoresis in SDS-agarose gels. With this technique the various DNA species present in a pulse-chase-labeled sample were separated, first in a nondenaturing neutral buffer and then under fully denaturing alkaline conditions (Fig. 3). In this analysis, upper forms of monomer (m1) and dimer (d1) duplex DNA, as identified in the first (neutral) dimension, migrated as single strands of 5 and 10 kb, respectively, in the second (alkaline) dimension, indicating that they do not contain any covalently closed turn-around forms of the viral termini. In contrast, the m2 and d2 forms migrated under alkaline conditions as 10- and 20-kb single strands, respectively, indicating that they have one turn-around terminus and one extended terminus. The monomer band which migrated fastest under neutral conditions, m3, migrated under alkaline conditions as either 10-kb single strands or as a species, mC, with a higher, variable mobility (previously observed in Fig. 2) and characterized as a covalent continuous strand. Introduction of a single random nick into such a circular 10-kb DNA molecule would produce a discrete linear 10-kb molecule, whereas introduction of a single random nick into a linear 10-kb DNA molecule would produce two fragments of variable sizes. The pattern seen in the m3 region of Fig. 3 suggested that such random nicks are common in this form, since there was a discrete 10-kb circular form, a discrete 10-kb linear form, and a smear of DNA extending down to the gel front. However, at present, we cannot rule out the possibility that some of the 10-kb linear forms have one covalently closed terminus and one correctly excised but protein-free terminus. Similarly, the

fastest-migrating form of dimer RF (d3) in the neutral dimension migrated in the alkaline dimension as either 20-kb single strands or 20-kb covalently closed circles (designated dC in Fig. 3). From the smear generated in the alkaline dimension from d3, m2, and d2, it would appear that a fraction of these molecular forms may also contain random nicks.

It appears, therefore, that at least large proportions of both the m3 and d3 forms are protein-free molecules with both termini in the turn-around configuration, confirming our conclusions reported elsewhere (7a). Such molecules are frequently present as intact covalently closed DNA loops but may also contain one or more randomly distributed nicks. Whether these nicks are present in infected cells or occur during the extraction procedure is not certain at present. Clearly, the generation of covalently closed DNA circles from linear, single-stranded input genomes indicates that the MVM replication scheme must include a ligation event of some kind.

The existence of such covalent continuous DNA molecules in vivo lends support to the modified rolling hairpin model (1, 2), which invokes a φX174-like topoisomerase. However, the features which make such a mechanism so advantageous for φX174, namely, that the necessary cleavages and ligations are coupled and energy independent and that the enzyme acts catalytically (9), seem of little consequence for MVM, especially since it appears to use the same protein but a less complex mechanism to process the other end of its genome. This fact suggests that one or more of the structures generated by the reaction may be critically important in the regulation of the replication cycle.

Nonequivalence of the two genomic termini. The various forms of monomer RF (m1 to m3) described in this study and elsewhere (7a) may act predominantly as substrates for different types of DNA synthesis. Thus, for example, it is easy to envisage that m1 forms would be ideally suited for virion strand synthesis (although they could also be used for a rather slow type of RF amplification), while m2 forms would appear to be particularly efficient substrates for rapid RF amplification through a dimer intermediate. Obviously, the forms of monomer RF which accumulate at different times during infection reflect, to some extent, the particular rate-limiting replication step prevailing at that time. Early in infection m1 forms may accumulate because, at this time, the ability to disrupt interstrand base pairing and form stable "rabbit-ear" structures at the genomic termini is rate limiting, while at later times the accumulation of turn-around forms may reflect a diminishing supply of the nicking protein or complex responsible for excising the genomic termini.

As originally presented, the modified rolling hairpin model (1, 2) predicted that extended and turn-around forms of the left-hand terminus should be generated in equimolar amounts. However, we found that, at the time of maximum RF DNA amplification (12 h after the release from aphidicolin), the termini of unit-length DNA molecules did not reflect these proportions. This result suggests that, if the topoisomerase model is correct, molecules with a turn-around configuration at the left-hand end of the genome must be metabolically more active than those with extended left-hand termini. To examine this aspect of replication in more detail, we analyzed the proportions of extended and turn-around termini present in unit-length molecules at different times during infection by using restriction endonucleases which cut to release separable fragments from each terminal conformation.

Restriction endonuclease analysis of immunoprecipitated DNA containing predominantly the m1 or m2 forms of the monomer confirmed the structures inferred from the two-dimensional gel analysis and showed that most of the m2 molecules have extended right-hand and turn-around left-hand termini, indicating that processing at each end of the molecule proceeds with different kinetics (Fig. 4). In the experiments shown, the duplexes were cut at the *Xba*I site, 807 nucleotides from the right end of the genome (Fig. 4, lanes 3, 4, and 5), or at the *Fsp*I site, 1,063 nucleotides from the left end (Fig. 4, lanes 6, 7, and 8). This step effectively blunted one end of the genome and allowed analysis of heterogeneity at the other end, but since the fragments being analyzed were large and of similar size, autoradiographic intensity closely reflected molarity, and quantitation was not complicated by such factors as molecular size, unrepresentative labeling of the palindromes, or nonlinearity of the film response. Immunoprecipitates enriched for the m1 form of the monomer produced digests containing predominantly the slower-mobility (extended) form of both termini (Fig. 4, lanes 3 and 6), while immunoprecipitates enriched for the m2 form of the monomer produced mostly the slower-mobility (extended) form of the right-hand terminus (Fig. 4, lane 7) but the faster-mobility (turn-around) form of the left-hand

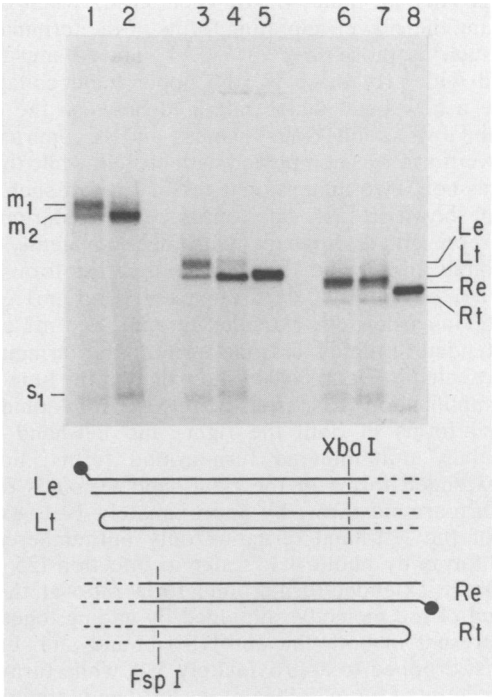

FIG. 4. Autoradiograph of a 1% agarose–SDS gel showing material immunoprecipitated with anti-NS-1 serum from cells labeled with $^{32}P_i$ for 1 h starting 10 h after the start of the S phase and then chased with cold medium for 1 h (lane 1) or 14 h (lane 2). Immunoprecipitates identical to those seen in lanes 1 and 2 were digested with *Xba*I (lanes 3 and 4, respectively) to demonstrate heterogeneity at the left end of the genome or with *Fsp*I (lanes 6 and 7, respectively) to demonstrate heterogeneity at the right end of the genome. Restriction digests containing a large amount of the upper form of one terminus or the other (equivalent to those shown in lanes 3 and 6) were digested with proteinase K and electrophoresed in lanes 5 and 8, respectively. The diagram beneath the gel illustrates the viral genome with its termini first in the extended configuration and then in the turn-around configuration and identifies the positions of the *Xba*I site at nucleotide 4343 and the *Fsp*I site at nucleotide 1062. Le, Left extended; Lt, left turnaround; Re, right extended; Rt, right turnaround.

terminus (Fig. 4, lane 4). In each case, when samples containing the slower-migrating forms of the terminal structures (such as those seen in Fig. 4, lanes 3 and 6) were digested with proteinase K, the upper band collapsed to produce a new band which migrated between the original upper and lower bands (Fig. 4, lanes 5 and 8), confirming that the slower form was complexed with protein while the faster form was not. Two-dimensional gel analysis of such digests (data not shown) in each case confirmed that faster-migrating forms represented duplexes with one covalently closed turn-around end, while the slower-migrating forms represented non-covalently closed duplexes. Thus, m1 contains two protein-associated, extended termini, and m2 contains one extended terminus and one turn-around terminus. The data presented in Figure 4 also show that, at the time of peak DNA amplification (12 h after the release from aphidicolin), extended forms of both the right- and left-hand termini substantially outnumbered turn-around forms; however, while extended forms of the right-hand terminus outnumbered turn-around forms by approximately 10:1, extended forms of the left-hand terminus only outnumbered turn-around forms by about 4:1. Later in infection (25 h post-release) the extended/turn-around form ratio at the right-hand end of the molecule, obtained by adding together the forms present in both the anti-NS-1-bound and -unbound fractions, dropped to approximately 5:1, while turn-around forms accounted for over 90% of the left-hand termini. Thus, turn-around forms of both genomic termini tend to accumulate as the infection proceeds, but at all times extended forms of the right-hand terminus vastly outnumber comparable forms of the left-hand terminus.

The nonequivalence in the rate with which extended forms of the right- and left-hand termini were generated suggests that, even if they are excised by the same endonuclease, excision of left-hand ends is a different, perhaps more complex, type of event, as compared with the processing of right-hand ends. However, as discussed above, the topoisomerase model predicts the generation of equivalent numbers of extended and turn-around forms of the left-hand end, but the accumulated unit-length molecules at no time reflected these proportions. Late in infection, depletion of nicking enzymes or replication machinery might easily lead to the observed preferential accumulation of turn-around forms of this terminus, but it is more difficult to explain their submolarity at the time of maximal RF DNA amplification and single-stranded DNA synthesis. Since most of the data presented in this paper clearly support the basic tenets of the modified rolling hairpin model (1, 2), we suggest that this apparent underrepresentation of turn-around forms of the left-hand end at times of peak DNA replication may well indicate that this type of intermediate is metabolically more active than the type with both termini in the extended configuration. If this is so, MVM may use a surprisingly complex mechanism to excise its left-hand end to promote the rapid regeneration of molecules with one turn-around terminus. According to the replication model, such molecules would be expected to permit fast and efficient amplification of the viral duplex RF DNA pool.

This work was supported by Public Health Service grants CA-16038 and AI-26109 from the National Institutes of Health. M.G. had financial support from the Institut National de la Santé et de la Recherche Medicale (France) and from the Association pour la Recherche sur le Cancer (France).

LITERATURE CITED

1. **Astell, C. R., M. B. Chow, and D. C. Ward.** 1985. Sequence analysis of the termini of virion and replicative forms of minute virus of mice DNA suggests a modified rolling hairpin model for autonomous parvovirus DNA replication. J. Virol. **54**:171–177.
2. **Astell, C. R., M. Thomson, M. B. Chow, and D. C. Ward.** 1983. Structure and replication of minute virus of mice DNA. Cold Spring Harbor Symp. Quant. Biol. **47**:751–762.
3. **Cotmore, S. F., and P. Tattersall.** 1986. Organization of the nonstructural genes of the autonomous parvovirus minute virus of mice. J. Virol. **58**:724–732.
4. **Cotmore, S. F., and P. Tattersall.** 1987. The autonomously replicating parvoviruses of vertebrates. Adv. Virus Res. **33**: 91–174.
5. **Cotmore, S. F., and P. Tattersall.** 1988. The NS-1 polypeptide of minute virus of mice is covalently attached to the 5′ termini of duplex replicative-form DNA and progeny single strands. J. Virol. **62**:851–860.
6. **Eisenberg, S., J. Griffith, and A. Kornberg.** 1977. φX174 cistron A protein is a multifunctional enzyme in DNA replication. Proc. Natl. Acad. Sci. USA **74**:3198–3202.
7. **Faust, E. A., and D. C. Ward.** 1979. Incomplete genomes of the parvovirus minute virus of mice: selective conservation of genome termini. J. Virol. **32**:276–292.

7a. **Gunther, M., and P. Tattersall.** 1988. The terminal protein of minute virus of mice is an 83 kilodalton polypeptide linked to specific forms of double-stranded and single-stranded viral DNA. FEBS Lett. **242**:22–26.

8. **Heintz, N. H., J. D. Milbrandt, K. S. Greisen, and J. L. Hamlin.** 1983. Cloning of the initiation region of a mammalian chromosomal replicon. Nature (London) **302**:439–441.
9. **Kornberg, A.** 1980. DNA replication. W. H. Freeman & Co., San Francisco.
10. **Roth, M. J., D. R. Brown, and J. Hurwitz.** 1984. Analysis of bacteriophage φX174 gene A protein-mediated termination and reinitiation of φX DNA synthesis. II. Structural characterization of the covalent φX A protein-DNA complex. J. Biol. Chem. **259**:10556–10568.
11. **Tattersall, P., and D. C. Ward.** 1976. Rolling hairpin model for replication of parvovirus and linear chromosomal DNA. Nature (London) **263**:106–109.
12. **Van Mansfield, A. D., P. D. Baas, and H. S. Jansz.** 1984. Gene A protein of bacteriophage φX174 is a highly specific single-strand nuclease and binds via a tyrosyl residue to DNA after cleavage. Adv. Exp. Med. Biol. **179**:221–230.